Aging Brain 5 (2024) 100111

Contents lists available at ScienceDirect

Aging Brain

journal homepage: www.elsevier.com/locate/nbas

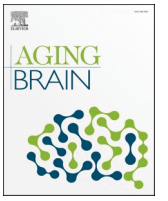

Pulsatility analysis of the circle of Willis

Henning U. Voss [a,b,*], Qolamreza R. Razlighi [c]

[a] Department of Radiology, Weill Cornell Medicine, New York, NY, USA
[b] Cornell MRI Facility, College of Human Ecology, Cornell University, Ithaca, NY, USA
[c] Quantitative Neuroimaging Laboratory, Brain Health Imaging Institute, Department of Radiology, Weill Cornell Medicine, New York, NY, USA

ARTICLE INFO

Keywords:
Brain Imaging
Circle of Willis
MRI
Cerebral Hemodynamics
Vascular Pulsatility
Cerebrospinal Fluid

ABSTRACT

Purpose: To evaluate the phenomenological significance of cerebral blood pulsatility imaging in aging research.
Methods: N = 38 subjects from 20 to 72 years of age (24 females) were imaged with ultrafast MRI with a sampling rate of 100 ms and simultaneous acquisition of pulse oximetry data. Of these, 28 subjects had acceptable MRI and pulse data, with 16 subjects between 20 and 28 years of age, and 12 subjects between 61 and 72 years of age. Pulse amplitude in the circle of Willis was assessed with the recently developed method of analytic phase projection to extract blood volume waveforms.
Results: Arteries in the circle of Willis showed pulsatility in the MRI for both the young and old age groups. Pulse amplitude in the circle of Willis significantly increased with age ($p = 0.01$) but was independent of gender, heart rate, and head motion during MRI.
Discussion and conclusion: Increased pulse wave amplitude in the circle of Willis in the elderly suggests a phenomenological significance of cerebral blood pulsatility imaging in aging research. The physiologic origin of increased pulse amplitude (increased pulse pressure vs. change in arterial morphology vs. re-shaping of pulse waveforms caused by the heart, and possible interaction with cerebrospinal fluid pulsatility) requires further investigation.

Introduction

Cerebrovascular pulsatility has gained significant importance as a research topic, primarily due to its potential impact on aging-related brain health. With advancing age, and in certain conditions such as chronic hypertension, the physical properties of the brain vasculature, and subsequently the vascular network, including its viscoelasticity, undergo changes [1–5]. These changes can lead to a reduction of the absorption of blood pressure pulsations, an increased impedance, and the potential for damage, including hemorrhagic stroke and microbleeds. Notably, small-scale changes that may not be evident in conventional imaging have attracted attention as potential contributors to conditions like dementia [6–8]. Furthermore, there is a growing body of evidence linking cerebrovascular health to various aspects of cognitive function and neurodegenerative diseases. For instance, aortic stiffness has been associated with cerebral small-vessel disease in hypertensive patients [9], cognitive decline correlates with the pulse wave velocity [10], and neurodegenerative diseases such as Alzheimer's disease are believed to be connected to cerebrovascular dysregulation [11–15]. Additionally, central artery stiffness has been reported to impact the perfusion of deep subcortical matter [16], central

* Corresponding author at: Cornell MRI Facility, College of Human Ecology, Cornell University, Martha Van Rensselaer Hall East, G305, 116 Reservoir Avenue, Ithaca, NY 14853-4401, USA.
E-mail address: hv28@cornell.edu (H.U. Voss).

https://doi.org/10.1016/j.nbas.2024.100111
Received 26 September 2023; Received in revised form 13 February 2024; Accepted 26 February 2024

arterial aging appears to be linked to an increased volume of white matter hyperintensities [17], and arterial stiffness is associated with beta-amyloid deposition in the elderly [18]. In a more indirect manner, the pressure gradient induced by arterial pulsatility could potentially serve as a driving force in the brain's paravascular waste clearance system [19,20], which plays a crucial role in brain health by facilitating the removal of metabolic waste products.

Therefore, it would be advantageous to directly image vascular changes in the brain. However, there are only limited *in vivo* options for imaging vascular dynamics in the human brain. Arterial spin labelling is probably the most advanced current method with the highest spatial resolution [21,22]. It provides quantitative blood flow values in the capillary bed, assuming steady flow [23]. In contrast, the important parameter of arterial compliance depends on the pulsatile component of the flow. It can be imaged for larger vessels locally with transcranial Doppler ultrasound [24,25]. Pulsatile flow components can also be imaged over the whole brain with 4D phase contrast angiography [26]. However, there has been recent progress in imaging pulsatility [27–36] in the brain with fast echo-planar imaging (EPI). It is important to note that in the main cerebral arteries, pulse wave velocity is typically higher in magnitude (up to about 12 m/s) [37] than blood flow velocity (about 30 to 100 cm/s; varies widely with age, cardiac phase, blood pressure, type of artery, and other factors [38,39].

In this contribution, we utilize the method of MRI hypersampling by analytic phase projection [40], which has been proven to reveal pulse waveforms in the main cerebral arteries. Importantly, this method can be seamlessly integrated into clinical MRI scans without the requirement for non-standard equipment or pulse sequences.

The region under study is the circle of Willis (COW), chosen for both pragmatic and scientific reasons. Pragmatically, the COW is easy to define in MRI, and for the sake of ultrafast imaging, it provides a suitable region with little inter-subject variability due to reproducible slice prescription. From a scientific standpoint, the COW holds a significant role in pulsatility, as it has been hypothesized to function as a pressure absorber mechanism that helps prevent damage to the cranial microvasculature and the blood–brain barrier [41]. However, it is worth noting that everything inside the skull pulsates in synchrony with the heartbeat [41–45], including cerebrospinal fluid, the cortical surface, and veins. The methods used in this study could potentially be useful for investigating pulsatility and pulse waves in other areas of the brain as well.

The research presented here is motivated by our enthusiasm for the exciting quest to better understand the aging human brain via biomedical imaging [46–60].

Materials and methods

Subjects

All participants were recruited using random market mailing within a 50-mile radius of Columbia University Irving Medical Center. Specifically, a marketing company provided a list of potential participants based on the requested demographics and geographical locations, and a questionnaire was sent to the identified individuals. All subjects gave their informed written consent prior to the scanning sessions and were compensated for their time spent taking part in this study. The experimental design of our study and the recruitment process were approved by Columbia University Institutional Review Board. Thirty-eight young and older but otherwise healthy participants (with cognitive scores within 2 standard deviations of the age-matched norm) between 20 and 72 years of age (24 female) were recruited. The MRI and pulse data were inspected for quality, and 28 subjects had acceptable MRI and pulse data. Specifically, the ten scans that could not be used for further analysis consisted of two scans that had an incorrect acquisition plane orientation, four scans that showed extreme head motion, and four scans that did not have usable pulse data. Of the remaining scans used for further analysis, 16 subjects were between 20 and 28 years of age (12 female) and 12 subjects between 61 and 72 years of age (5 female).

Imaging

Subjects were imaged using a 3 Tesla Siemens Magnetom Prisma scanner equipped with an 80 mT/m gradient system with a T_2*-weighted ultrafast echo-planar imaging (EPI) sequence (repetition time = 100 ms, echo time = 35 ms, flip angle = 62°, field-of-view of 22 cm, matrix size of 100 × 100, and slice thickness of 3 mm) with simultaneous and synchronized acquisition of pulse oximetry data from the index finger of the left hand. In addition, time-of-flight angiography images were acquired to allow for accurate slice positioning of the EPI sequence. Using sagittal, coronal, and axial views of the angiogram, the MRI operator was carefully placing a single EPI imaging slice through the center of the COW, attempting to cover it as much as possible. This slice was imaged with 3000 repetitions totaling 5 min scan time. This procedure was repeated for a mid-sagittal slice including parts of the fourth ventricle.

Pulse waveform analysis

Preprocessing of raw MRI data:

The first fMRI image of each subject was used as an anchor to which all subsequent 2999 images were aligned to by an intensity-based rigid image registration algorithm (MATLAB's imregister function, which uses a regular step gradient descent optimizer. The minimum step size was set to 10^{-3}.). The EPI time series were detrended with a zero-lag high pass filter with a cutoff at 20 s, corresponding to 200 data points.

Preprocessing of pulse oximetry data

The pulse oximetry signals were filtered with a zero-lag lowpass filter with a cutoff at 1.5 Hz to enhance pseudo-periodicity [61–63] of the pulse signal, and to remove noise.

Estimation of pulse wave form and amplitude

For each subject, MRI pulse waveforms were extracted from the EPI-MRI data by analytic phase projection (APP) [40,64,65]. APP is a generalized form of retrospective gating. It overcomes the arbitrary limitation that the phase within an inter-beat interval is assumed to increase linearly: In APP, the phase of the pulse oximetry signal is estimated from the analytic phase of the pulse oximetry signal via a Hilbert transform. Thus, it can be nonlinear, leading to a more accurate gating for variable inter-beat intervals [66]. Then, each MRI data point is mapped to its corresponding phase, leading to a reordering of MRI data points in time, analogously to retrospective gating. Both retrospective gating and APP increase the number of data points during one cardiac cycle; it is equal to the total number of sampled MRI images, N (here, $N = 3000$). This provides a highly oversampled cardiac phase. This oversampling improves waveform estimation by partially averaging out factors that limit the temporal sampling accuracy. These factors include temporal blurring of the signal by the EPI readout time and estimation errors of the Hilbert phase. The pulse oximetry signals were then shifted in time to match the MRI acquisition sample times. The amount of shift was estimated by searching for the maximum average pulse signal amplitude in the hypersampled MRI data. The average pulse signal amplitude was averaged from the amplitudes in each voxel in the brain, by using a hand-drawn mask that excluded ventricles and skull areas. Finally, pulse waveforms were estimated by smoothing the hypersampled MRI signal with a zero-lag filter, retaining six cycles per cardiac cycle. For the display of waveforms in Fig. 1, waveforms were foot-to-foot normalized, after the sign of the waveform was determined by computation of the Q-value, a measure to assess the skewness of temporal correlations in a time series [67]. For negative Q, the sign of the waveform was inverted. This procedure was used to solve the problem that the sign of the MRI signal is not pre-determined, and this way the systolic upstroke appeared to have positive slope.

Motion assessment

For each subject, head motion was quantified by the standard deviation of the rotation angle of the rigid transformation used for motion correction, using MATLAB's imregtform function. In order to exclude the possibility that the amount of head motion during MRI scanning biased pulsatility measures, this parameter was included as a covariate in the statistical analysis.

Statistics

Two circular regions of interest (ROIs) were defined for each fMRI data set (Fig. 1): 1. An ROI centered at the COW, and 2. an ROI centered in a brain area nearby without noticeable pulsatility, used as baseline. The MRI pulse amplitude was computed for these ROIs as the average of the differences between the maximum and minimum waveform value. In the COW, this amplitude was then divided by the median amplitude from the baseline ROI. To evaluate the age dependence of pulsatility, a multiple regression analysis was performed with MRI pulse amplitudes in the COW as dependent variable and age, heart rate, motion, and gender as independent variables. Gender was used as a categorical variable. In addition, another multiple regression analysis was used to test for the possibility that the baseline ROI depends on any of the three independent variables. The same analysis was performed on the maximum amplitude voxel in the fourth ventricle, and normalized to a baseline ROI of 13 voxels in the center of the pons, which generally showed very low pulsatility amplitude.

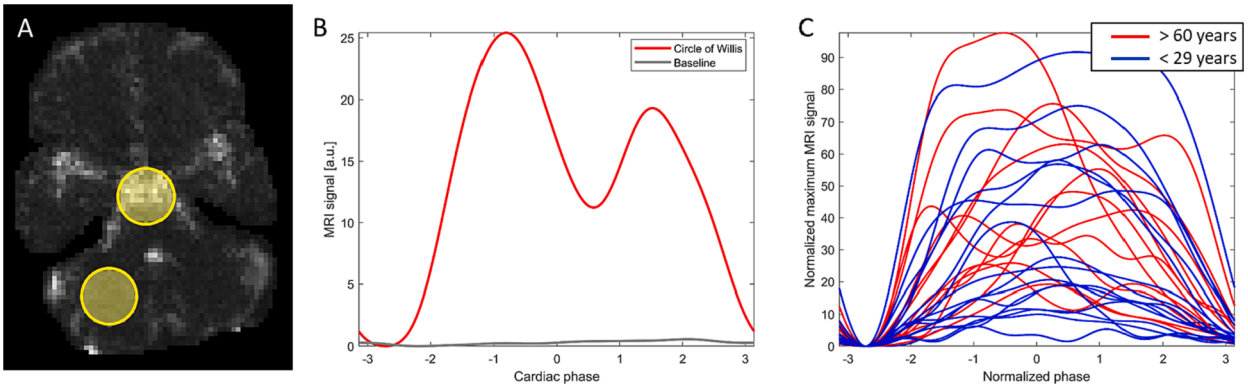

Fig. 1. MRI pulse waves. A) The square root of MRI pulse wave amplitudes over the brain slice acquired with ultrafast MRI, for a single subject. The region of interest for the analysis of the circle of Willis and the baseline region without dominant pulsatility are highlighted. B) The maximum-amplitude MRI pulse wave in the circle of Willis shows the characteristic systolic upstroke starting at around phase value −2.5 rad. In addition, the maximum-amplitude baseline signal is shown in gray. C) Maximum-amplitude waveforms for all subjects, baseline-normalized.

Results

Pulse amplitude maps could reliably be obtained from all 28 subjects and showed pulsatility in the circle of Willis, parts of the middle cerebral arteries, arteries in the scalp, and other regions, including spaces filled with cerebrospinal fluid (CSF). An example pulse amplitude map is shown in Fig. 1 for a single subject. Estimates of pulse waveforms often showed characteristic features such as the systolic upstroke and dicrotic notch (Fig. 1C), but overall show significant inter-subject variability.

A multiple regression analysis revealed that pulse amplitude in the COW increased with age ($p = 0.01$) but was not significantly dependent on heart rate, gender, or head motion during MRI. In the baseline region, pulse amplitude did not depend on age, heart rate, motion, or gender. The statistics is summarized in Table 1, and the increase of pulse amplitude with age in the COW is shown in Fig. 2.

Discussion

Our interpretation of age-related increase of fMRI derived pulse wave amplitude in the circle of Willis is as follows. In general, arterial blood flow consists of two components: The steady and the pulsatile flow [68–70]. Outside the capillary bed [71], the former is mainly affected by peripheral vascular resistance, while the latter is mainly affected by arterial stiffness. After the age of 60, increases in blood pressure are primarily attributable to an increase of systolic pressure, leading to a rapid increase of pulse pressure, the difference between systolic and diastolic pressure [72]. We suggest that increased pulse pressure in cerebral arteries causes increased pulse amplitude in the COW, because the pulsatile blood flow experiences a relatively greater increase than the steady flow. An alternative explanation for larger pulse wave amplitudes could be that the arterial compliance, the ratio of blood volume and blood pressure, increases with age in the circle of Willis. However, due to the lack of information about intracranial blood pressure, and the fact that this explanation would contradict the general trend of an increase of arterial stiffness with age, this seems to be less likely.

The observed variability of waveform shapes across subjects is likely partially related to the known interindividual variation of COW structure and function in the general population, including hypoplastic posterior communicating arteries and duplicated/missing communicating arteries. For an overview of COW variance studies see Vrselja et al. [41] and the later *meta*-analysis by Jones et al. [73]. In one study, a complete COW was identified in less than half of the population [74]. The variability in pulse waveforms is accompanied by interindividual variability of pulsatility amplitude and anatomy in the present sample: Supplementary Fig. 1 shows pulse amplitude maps for the scanned slice through the COW, and Supplementary Fig. 2 MRA maximum-intensity projections of all subjects.

The COW is embedded into the subarachnoid space, which is also filled with CSF. We cannot exclude that the CSF in this space might pulsate itself. For another CSF filled space, the aqueduct, it is known that CSF pulsatility increases with age in healthy subjects [75] (but also see references [76–81] for missing or opposite age effects on cerebral CSF pulsatility). In our study, it was difficult to separate possible CSF contributions to pulsatility with the present resolution of the pulsatility scan. Therefore, to assess the age dependence of CSF pulsatility in this subject sample, an analysis of the fourth ventricle, scanned in mid-sagittal orientation but otherwise with identical parameters as the COW MRIs, was performed. It is plausible that pulsatility of the CSF in small CSF filled spaces can be picked up with the same method of analytic phase projection. A highly significant age dependence of CSF pulsatility was observed (Supplementary Fig. S3A), and the CSF pulse waveforms showed a pronounced separation between the two age groups, too (Supplementary Fig. S3B). Therefore, this result, obtained with our specific protocol and in this specific group of subjects, needs to be considered in the interpretation of pulsatility of the COW. The question whether CSF pulsation is partially responsible for the here observed age increase of pulsatility could be better assessed with blood-flow sensitive imaging such as phase-contrast MRI [82]. This would allow for a separation of pulsatility into fast (blood) and slow (CSF) motion components, and is planned in our future research.

It is an open question whether the increase in waveform amplitude is due to a change of the wave form before it enters the brain, due to a change inside the cerebral arteries, or due to an altered wave reflection at the arteriole/capillary level. A more thorough investigation would have to involve the measurement of wave forms at the aortic or carotid level [83,84], and MRI of larger brain regions. It is neither clear from the present data if an actual re-shaping of the waves or an amplification, or a combined effect thereof, takes place [85–90]. For a detailed analysis of wave forms, one would have to acquire data with higher spatial resolution that would allow for probing specific vessels rather than the *average* pulse amplitude in the circle of Willis. With faster imaging methods and higher field MRI [91–95], studies like these are now within reach and subject of further research.

This MRI experiment was not specifically designed to investigate pulsatility in the circle of Willis, and follows up on the incidental finding of pulsatility using fast fMRI [96–99]. As such, it was not optimized for detecting pulsatility, and the study design and MRI

Table 1
Multiple linear regression analysis. Number of observations: 28, Error degrees of freedom: 23. COW: Root Mean Squared Error: 3.33, R-squared: 0.261, Adjusted R-Squared: 0.132, F-statistic vs. constant model: 2.03, p-value = 0.124. Baseline: Root Mean Squared Error: 0.11, R-squared: 0.113, Adjusted R-Squared: -0.0418, F-statistic vs. constant model: 0.729, p-value = 0.581

	Circle of Willis			Baseline		
Variable	**Estimate**	**t-value**	**p-value**	**Estimate**	**t-value**	**p-value**
Intercept	7.7	1.5	0.1	0.3	1.8	0.09
Age	0.1	2.8	**0.01**	−0.0007	−0.6	0.6
Heart rate	−0.04	−0.5	0.6	0.0005	0.2	0.9
Gender	−1.5	−1.0	0.3	−0.05	−1.1	0.3
Motion	−1286	−1.3	0.2	11	0.3	0.7

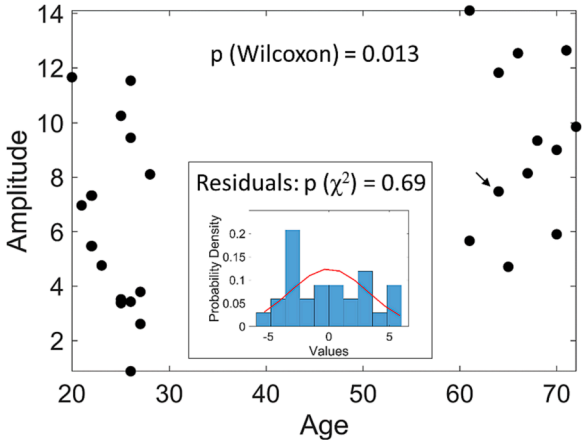

Fig. 2. Increase of mean pulse amplitudes with age in the circle of Willis. The two age groups have different mean value with a p-value of 0.013 (post-hoc non-parametric Wilcoxon test). The amplitudes used here were normalized by the median baseline amplitude for each subject. The subject of Fig. 1 is marked with an arrow. The inset shows the distribution of the residuals of a linear regression fit and the p-value for the hypothesis that the residuals are not normally distributed.

parameters chosen here might not all be optimal for MRI studies of cerebral pulsatility. Therefore, we are concluding the discussion by reviewing some specific considerations for MRI studies of pulsatility in the circle of Willis.

The pulse wave from the heart to the finger experiences a different distance and vasculature than the pulse wave from the heart to the circle of Willis. The temporal shift between signals measured on the finger with pulse oximetry and the signal measured with MRI [98] in the circle of Willis should therefore show interindividual variability, which might contain useful information. For example, increased pulse wave velocities caused by increased arterial stiffness would affect this shift. However, our technical setup with a lack of absolute reference times precluded such an analysis.

The flip angle of 62° was not optimized to be maximally flow sensitive. A flip angle of 90° would be more suitable to emphasize inflowing blood and would possibly result in an increase of pulse wave amplitudes [100]. In order to develop pulsatility imaging of the circle of Willis, with its combination of blood vessels of different diameters, as a diagnostic tool, a thorough study of the effects of MRI parameters could be worthwhile to undertake. Imaging parameters such as resolution, flip angle, and echo times will have to be optimized to maximize sensitivity of such a tool.

Impressive progress in vascular pulsatility imaging has been made with phase-contrast angiography and related fast MRI methods [83,101–109]. We believe that high-resolution 4D phase contrast, combined with high-resolution angiographic imaging, and peripheral blood pressure and pulse wave velocity measurements, will provide a powerful approach to investigate further the cause and effects of age- and disease-related changes of pulsatility in this region.

The observed pulsatility in the circle of Willis was not strong enough to accurately estimate the cardiac phase from the signal itself, which was overcome by estimating the phase with analytic phase projection [40]. However, for sufficiently strong signals, it is possible to estimate the phase from the MRI data itself [98,110–112], which could increase accuracy of waveform estimates. Such an approach could pave the way to a more detailed analysis of pulse waveform shapes and their potential interpretation.

This study was designed to compare young and old subjects with each other [84]. However, it is known from sonography studies that in men, carotid artery distensibility and compliance begin to decrease around 30 years of age [113]. Our study does not catch potential changes in cerebrovascular physiology in this age group. In order to investigate potential precursors of increased risk of future cerebrovascular disease [114], it would be worthwhile to include the cohort of the 30 to 60 years old, too.

Conclusion

We have evaluated the significance of cerebral blood pulsatility imaging in the circle of Willis and investigated its changes with age. We showed that the arteries of the circle of Willis exhibit MRI-pulsatility for both the young and old age groups, and that pulse amplitude significantly increases with age. This suggests a phenomenological significance of cerebral blood pulsatility imaging in aging research. However, the physiologic origin of increased pulse amplitude requires further investigation.

Data sharing

The MRI data is available upon request for scientific researchers. The APP algorithm has been published before [40] and is also available here:
www.mathworks.com/matlabcentral/fileexchange/68807-pwp.

Author contributions

H. U. Voss: Data curation; Formal analysis; Investigation; Methodology; Software; Writing – original draft. O. R. Razlighi Conceptualization; Data curation; Investigation; Project administration; Resources; Supervision; Writing – review & editing.

CRediT authorship contribution statement

Henning U. Voss: Writing – review & editing, Writing – original draft, Validation, Software, Methodology, Investigation, Formal analysis. **Qolamreza R. Razlighi:** Writing – review & editing, Writing – original draft, Supervision, Resources, Project administration, Investigation, Funding acquisition, Data curation, Conceptualization.

Declaration of competing interest

The authors declare the following financial interests/personal relationships which may be considered as potential competing interests: The corresponding author is the inventor of patent WO 2019/199960A1, awarded to Cornell University, that describes the method of hypersampling used in this work.

Acknowledgments

The authors acknowledge help from David Parker and Amirreza Sedaghat. Also, the comments of the reviewers are highly appreciated.

Appendix A. Supplementary data

Supplementary data to this article can be found online at https://doi.org/10.1016/j.nbas.2024.100111.

References

[1] Henry Feugeas MC, De Marco G, Peretti II, Godon-Hardy S, Fredy D, Claeys ES. Age-related cerebral white matter changes and pulse-wave encephalopathy: Observations with three-dimensional MRI. Magn Reson Imaging 2005;23(9):929–37.
[2] Guyton AC, Hall JE. Textbook of Medical Physiology. 11th edn. Saunders/Elsevier: Philadelphia, Pa; 2006.
[3] Laurent S, Cockcroft J, Van Bortel L, Boutouyrie P, Giannattasio C, Hayoz D, et al. Expert consensus document on arterial stiffness: methodological issues and clinical applications. Eur Heart J 2006;27(21):2588–605.
[4] O'Rourke MF, Hashimoto J. Mechanical factors in arterial aging: A clinical perspective. J Am Coll Cardiol 2007;50(1):1–13.
[5] Tarumi T, Ayaz Khan M, Liu J, Tseng BY, Parker R, Riley J, et al. Cerebral hemodynamics in normal aging: central artery stiffness, wave reflection, and pressure pulsatility. J Cerebr Blood F Met 2014;34(6):971–8.
[6] Gorelick PB, Scuteri A, Black SE, DeCarli C, Greenberg SM, Iadecola C, et al. Vascular contributions to cognitive impairment and dementia - A statement for healthcare professionals from the American Heart Association/American Stroke Association. Stroke 2011;42(9):2672–713.
[7] de Roos A, van der Grond J, Mitchell G, Westenberg J. Magnetic resonance imaging of cardiovascular function and the brain: Is dementia a cardiovascular-driven disease? Circulation 2017;135(22):2178–95.
[8] Levin RA, Carnegie MH. Celermajer DS. An emerging therapeutic target for dementia. Front Neurosci: Pulse pressure; 2020. p. 14.
[9] Henskens LHG, Kroon AA, van Oostenbrugge RJ, Gronenschild EHBM, Fuss-Lejeune MMJJ, Hofman PAM, et al. Increased aortic pulse wave velocity is associated with silent cerebral small-vessel disease in hypertensive patients. Hypertension 2008;52(6):1120–6.
[10] Rabkin SW. Arterial stiffness: Detection and consequences in cognitive impairment and dementia of the elderly. J Alzheimers Dis 2012;32(3):541–9.
[11] Iadecola C, Gorelick PB. Converging pathogenic mechanisms in vascular and neurodegenerative dementia. Stroke 2003;34(2):335–7.
[12] Iadecola C. Neurovascular regulation in the normal brain and in Alzheimer's disease. Nat Rev Neurosci 2004;5(5):347–60.
[13] Iadecola C. The pathobiology of vascular dementia. Neuron 2013;80(4):844–66.
[14] Li Y, Rusinek H, Butler T, Glodzik L, Pirraglia E, Babich J, et al. Decreased CSF clearance and increased brain amyloid in Alzheimer's disease. Fluids Barriers CNS 2022;19(1).
[15] Mehta NH, Suss RA, Dyke JP, Theise ND, Chiang GC, Strauss S, et al. Quantifying cerebrospinal fluid dynamics: A review of human neuroimaging contributions to CSF physiology and neurodegenerative disease. Neurobiol Dis 2022;170.
[16] Tarumi T, Shah F, Tanaka H, Haley AP. Association between central elastic artery stiffness and cerebral perfusion in deep subcortical gray and white matter. Am J Hypertens 2011;24(10):1108–13.
[17] Tarumi T, Khan MA, Liu J, Tseng BM, Parker R, Riley J, et al. Cerebral hemodynamics in normal aging: central artery stiffness, wave reflection, and pressure pulsatility. J Cereb Blood Flow Metab 2014;34(6):971–8.
[18] Hughes TM, Kuller LH, Barinas-Mitchell EJM, Mackey RH, McDade EM, Klunk WE, et al. Pulse wave velocity is associated with beta-amyloid deposition in the brains of very elderly adults. Neurology 2013;81(19):1711–8.
[19] Jessen NA, Munk ASF, Lundgaard I, Nedergaard M. The glymphatic system: A beginner's guide. Neurochem Res 2015;40(12):2583–99.
[20] Bacyinski A, Xu MS, Wang W, Hu JN. The paravascular pathway for brain waste clearance: Current understanding, significance and controversy. Front Neuroanat 2017;11.
[21] Wong EC, Buxton RB, Frank LR. Quantitative perfusion imaging using arterial spin labeling. Neuroimag Clin N Am 1999;9(2):333–42.
[22] Wolf RL, Detre JA. Clinical neuroimaging using arterial spin-labeled perfusion magnetic resonance imaging. Neurotherapeutics 2007;4(3):346–59.
[23] Dyke JP. Perfusion Imaging. In: Holodny A, editor. Functional Neuroimaging: A Clinical Approach. Informa Healthcare USA Inc: New York; 2008. p. 249–72.
[24] Aaslid R, Markwalder TM, Nornes H. Non-invasive transcranial doppler ultrasound recording of flow velocity in basal cerebral-arteries. J Neurosurg 1982;57(6):769–74.
[25] Hashimoto J, Westerhof BE, Ito S. Carotid flow augmentation, arterial aging, and cerebral white matter hyperintensities: comparison with pressure augmentation. Arterioscl Throm Vas 2018;38(12):2843–53.

[26] Frydrychowicz A, Francois CJ, Turski PA. Four-dimensional phase contrast magnetic resonance angiography: Potential clinical applications. Eur J Radiol 2011; 80(1):24–35.
[27] Dagli MS, Ingeholm JE, Haxby JV. Localization of cardiac-induced signal change in fMRI. Neuroimage 1999;9(4):407–15.
[28] Chang C, Cunningham JP, Glover GH. Influence of heart rate on the BOLD signal: The cardiac response function. Neuroimage 2009;44(3):857–69.
[29] Voss HU, Dyke JP, Ballon DJ, Schiff ND, Tabelow K. Magnetic Resonance Advection Imaging (MRAI) depicts vascular anatomy. Conference abstract OHBM. Hum Brain Mapp 2015::2436.
[30] Voss HU, Dyke JP, Ballon DJ. Mapping cerebrovascular dynamics with MR advection imaging (MRAI): Estimation bias and image reconstruction challenges. Conference abstract ICERM - Computational and Analytical Aspects of Image Reconstruction. 2015.
[31] Voss HU, Dyke JP, Tabelow K, Ballon DJ, Schiff ND. Magnetic resonance advection imaging (MRAI): Sensitivity to pulsatile flow. *Conference abstract BRAIN/PET* 2015; 2015: 141.
[32] Voss HU, Dyke JP, Tabelow K, Schiff ND, Ballon DJ. Mapping cerebrovascular dynamics with magnetic resonance advection imaging (MRAI): Modeling challenges and estimation bias. Conference abstract Meeting of the Society for Neuroscience. 2015.
[33] Bianciardi M, Toschi N, Polimeni JR, Evans KC, Bhat H, Keil B, et al. The pulsatility volume index: An indicator of cerebrovascular compliance based on fast magnetic resonance imaging of cardiac and respiratory pulsatility. Philos T R Soc A 2016;374:1–19.
[34] Voss HU, Dyke JP, Tabelow K, Schiff ND, Ballon DJ. Magnetic resonance advection imaging of cerebrovascular pulse dynamics. J Cereb Blood Flow Metab 2017;37(4):1223–35.
[35] Hubmer S, Neubauer A, Ramlau R, Voss HU. On the parameter estimation problem of magnetic resonance advection imaging. Inverse Problems and Imaging 2018;12(1):175–204.
[36] Hubmer S, Neubauer A, Ramlau R, Voss HU. A conjugate-gradient approach to the parameter estimation problem of magnetic resonance advection imaging. Inverse Probl Sci En 2020;28(8):1154–65.
[37] Giller CA, Aasli DR. Estimates of pulse-wave velocity and measurement of pulse transit-time in the human cerebral-circulation. Ultrasound Med Biol 1994;20 (2):101–5.
[38] Sorteberg W, Langmoen A, Lindegaard KF, Nornes H. Side-to-side differences and day-to-day variations of transcranial doppler parameters in normal subjects. J Ultrasound Med 1990;9(7):403–9.
[39] Ringelstein EB, Kahlscheuer B, Niggemeyer E, Otis SM. Transcranial doppler sonography - anatomical landmarks and normal velocity values. Ultrasound Med Biol 1990;16(8):745–61.
[40] Voss HU. Hypersampling of pseudo-periodic signals by analytic phase projection. Comput Biol Med 2018;98:159–67.
[41] Vrselja Z, Brkic H, Mrdenovic S, Radic R, Curic G. Function of circle of Willis. J Cerebr Blood F Met 2014;34(4):578–84.
[42] Parker KH. An introduction to wave intensity analysis. Med Biol Eng Comput 2009;47(2):175–88.
[43] Wagshul ME, Eide PK, Madsen JR. The pulsating brain: A review of experimental and clinical studies of intracranial pulsatility. Fluids Barriers CNS 2011;8(1): 5.
[44] Holdsworth SJ, Rahimi MS, Ni WW, Zaharchuk G, Moseley ME. Amplified magnetic resonance imaging (aMRI). Magn Reson Med 2016;75(6):2245–54.
[45] Terem I, Ni WW, Goubran M, Rahimi MS, Zaharchuk G, Yeom KW, et al. Revealing sub-voxel motions of brain tissue using phase-based amplified MRI (aMRI). Magn Reson Med 2018;80(6):2549–59.
[46] Ferris SH, Farkas I, Alavi A, Deleon M, Rampal S, Reisberg B, et al. Regional brain metabolism in aging and senile dementia determined by positron emission tomography. Age 1980;3(4):113.
[47] Deleon MJ, Ferris SH, George AE, Christman DR, Fowler JS, Gentes C, et al. Positron emission tomographic studies of aging and Alzheimer-disease. Am J Neuroradiol 1983;4(3):568–71.
[48] Deleon MJ, George AE, Miller J, Kluger A, Gianutsos J, Klinger A, et al. Longitudinal and PET studies of leukoencephopathy in normal aging. Am J Neuroradiol 1987;8(5):955.
[49] Leenders KL, Perani D, Lammertsma AA, Heather JD, Buckingham P, Healy MJR, et al. Cerebral blood-flow, blood-volume and oxygen utilization - normal values and effect of age. Brain 1990;113:27–47.
[50] Cotrina ML, Nedergaard M. Astrocytes in the aging brain. J Neurosci Res 2002;67(1):1–10.
[51] Schuitemaker A, Boellaard R, van der Flier WM, Kropholler MA, Windhorst AD, Barkhof F, et al. Microglial activation in healthy aging. Neuroimage 2010;52: S32–.
[52] Mitchell GF, van Buchem MA, Sigurdsson S, Gotal JD, Jonsdottir MK, Kjartansson O, et al. Arterial stiffness, pressure and flow pulsatility and brain structure and function: the Age Gene/Environment Susceptibility - Reykjavik Study. *Brain* 2011;134:3398–407.
[53] Blum S, Habeck C, Steffener J, Razlighi Q, Stern Y. Functional connectivity of the posterior hippocampus is more dominant as we age. Cogn Neurosci 2014;5 (3–4):150–9.
[54] Kress BT, Iliff JJ, Xia MS, Wang MH, Wei HLS, Zeppenfeld D, et al. Impairment of paravascular clearance pathways in the aging brain. Ann Neurol 2014;76(6): 845–61.
[55] Gazes Y, Bowman FD, Razlighi QR, O'Shea D, Stern Y, Habeck C. White matter tract covariance patterns predict age-declining cognitive abilities. Neuroimage 2016;125:53–60.
[56] Liu XQ, Gerraty RT, Grinband J, Parker D, Razlighi QR. Brain Atrophy Can Introduce Age-Related Differences in BOLD Response. Hum Brain Mapp 2017;38(7): 3402–14.
[57] Butler T, Deshpande A, Harvey P, Li Y, Rusinek H, Pirraglia E, et al. Precisely-measured hydration status correlates with hippocampal volume in healthy older adults. Am J Geriatr Psychiatry 2019;27(6):653–4.
[58] Habeck C, Gazes Y, Razlighi Q, Stern Y. Cortical thickness and its associations with age, total cognition and education across the adult lifespan. PLoS One 2020; 15(3).
[59] Butler T, Glodzik L, Wang XH, Xi K, Li Y, Pan H, et al. Positron Emission Tomography reveals age-associated hypothalamic microglial activation in women. Sci Rep 2022;12(1).
[60] Zhou LD, Li Y, Sweeney EM, Wang XH, Kuceyeski A, Chiang GC, et al. Association of brain tissue cerebrospinal fluid fraction with age in healthy cognitively normal adults. Front Aging Neurosci 2023;15.
[61] Cohen L. What is a multicomponent signal? *ICASSP-92 -International Conference on Acoustics, Speech, and Signal Processing* 1992; 1-5: E113-E116.
[62] Sethares WA. Repetition and pseudo-periodicity. Tatra Mt Math Publ 2001;23:1–16.
[63] Jiang HX, Zhang K, Wang JY, Wang XY, Huang PF. Anomaly detection and identification in satellite telemetry data based on pseudo-period. Appl Sci-Basel 2020;10(1).
[64] Voss HU. Intracranial pulse waves derived from dynamic MRI. Conference abstract Allen Workshop BioImage Informatics. 2019.
[65] Voss HU, Dyke JP, Ballon DJ, Gupta A. MRI pulse wave profiles of cerebral arteries. Proceedings of the International Society for Magnetic Resonance in Medicine 2019:3247.
[66] Cysarz D, Porta A, Montano N, Leeuwen PV, Kurths J, Wessel N. Quantifying heart rate dynamics using different approaches of symbolic dynamics. Eur Phys J-Spec Top 2013;222(2):487–500.
[67] Theiler J, Eubank S, Longtin A, Galdrikian B, Farmer JD. Testing for Nonlinearity in Time-Series - the Method of Surrogate Data. Phys D 1992;58(1–4):77–94.
[68] Fung YC. Biomechanics: Circulation. 2nd edn. New York: Springer; 1997.
[69] Zamir M. The Physics of Pulsatile Flow. New York: AIP Press; Springer; 2000.
[70] Li JKJ. Dynamics of the Vascular System. River Edge, N.J.: World Scientific; 2004.
[71] Zhang Y, Lacolley P, Protogerou AD, Safar ME. Arterial stiffness in hypertension and function of large arteries. Am J Hypertens 2020;33(4):291–6.
[72] Franklin SS. Hypertension in older people: Part 1. J Clin Hypertens (Greenwich) 2006;8(6):444–9.

[73] Jones JD, Castanho P, Bazira P, Sanders K. Anatomical variations of the circle of Willis and their prevalence, with a focus on the posterior communicating artery: A literature review and meta-analysis. Clin Anat 2021;34(7):978–90.
[74] Krabbe-Hartkamp MJ, van der Grond J, de Leeuw FE, de Groot JC, Algra A, Hillen B, et al. Circle of Willis: Morphologic variation on three-dimensional time-of-flight MR angiograms. Radiology 1998;207(1):103–11.
[75] Sartoretti T, Wyss M, Sartoretti E, Reischauer C, Hainc N, Graf N, et al. Sex and age dependencies of aqueductal cerebrospinal fluid dynamics parameters in healthy subjects. Front Aging Neurosci 2019;11.
[76] Lokossou A, Metanbou S, Gondry-Jouet C, Balédent O. Extracranial versus intracranial hydro-hemodynamics during aging: a PC-MRI pilot cross-sectional study. Fluids Barriers CNS 2020;17(1).
[77] Sahoo P, Kollmeier JM, Wenkel N, Badura S, Gärtner J, Frahm J, et al. CSF and venous blood flow from childhood to adulthood studied by real-time phase-contrast MRI. Child Nerv Syst 2024.
[78] Daners MS, Knobloch V, Soellinger M, Boesiger P, Seifert B, Guzzella L, et al. Age-specific characteristics and coupling of cerebral arterial inflow and cerebrospinal fluid dynamics. PLoS One 2012;7(5).
[79] Oner Z, Kahraman AS, Kose E, Oner S, Kavakli A, Cay M, et al. Quantitative evaluation of normal aqueductal cerebrospinal fluid flow using phase-contrast cine MRI according to age and sex. Anatom Rec Adv Integr Anat Evol Biol 2017;300(3):549–55.
[80] Ünal Ö, Kartum A, Avcu S, Etlik Ö, Arslan H, Bora A. Cine phase-contrast MRI evaluation of normal aqueductal cerebrospinal fluid flow according to sex and age. Diagn Interv Radiol 2009;15(4):227–31.
[81] Stoquart-ElSankari S, Balédent O, Gondry-Jouet C, Makki M, Godefroy O, Meyer ME. Aging effects on cerebral blood and cerebrospinal fluid flows. J Cereb Blood Flow Metab 2007;27(9):1563–72.
[82] Pelc NJ, Herfkens RJ, Shimakawa A, Enzmann DR. Phase contrast cine magnetic resonance imaging. Magn Reson Q 1991;7(4):229–54.
[83] Wink C, Ferrazzi G, Bassenge JP, Flassbeck S, Schmidt S, Schaeffter T, et al. 4D flow imaging with 2D-selective excitation. Magn Reson Med 2019;82(3):886–900.
[84] Fico BG, Miller KB, Rivera-Rivera LA, Corkery AT, Pearson AG, Eisenmann NA, et al. The impact of aging on the association between aortic stiffness and cerebral pulsatility index. Front Cardiovasc Med 2022;9.
[85] Laxminarayan S. Calculation of forward and backward waves in the arterial system. Med Biol Eng Comput 1979;17(1):130.
[86] Merillon JP, Lebras Y, Chastre J, Lerallut JF, Motte G, Fontenier G, et al. Forward and backward waves in the arterial system, their relationship to pressure waves form. Eur Heart J 1983;4:13–20.
[87] Westerhof BE, van den Wijngaard JP, Murgo JP, Westerhof N. Location of a reflection site is elusive - Consequences for the calculation of aortic pulse wave velocity. Hypertension 2008;52(3):478–83.
[88] Tyberg JV, Bouwmeester JC, Shrive NG, Wang JJ. CrossTalk opposing view: Forward and backward pressure waves in the arterial system do not represent reality. J Physiol-London 2013;591(5):1171–3.
[89] Westerhof N, Westerhof BE. CrossTalk proposal: Forward and backward pressure waves in the arterial system do represent reality - Rebuttal from Nico Westerhof and Berend E Westerhof. J Physiol-London 2013;591(5):1175.
[90] Manoj R, Kiran VR, Nabeel PM, Sivaprakasam M, Joseph J. Separation of forward-backward waves in the arterial system using multi-gaussian approach from single pulse waveform. *243rd Annual International Conference of the IEEE Engineering in Medicine & Biology Society (EMBC)* 2021: 5547-5550.
[91] Moeller S, Yacoub E, Olman CA, Auerbach E, Strupp J, Harel N, et al. Multiband multislice GE-EPI at 7 Tesla, with 16-fold acceleration using partial parallel imaging with application to high spatial and temporal whole-brain fMRI. Magn Reson Med 2010;63(5):1144–53.
[92] Webb AJS, Simoni M, Mazzucco S, Kuker W, Schulz U, Rothwell PM. Increased cerebral arterial pulsatility in patients with leukoaraiosis Arterial stiffness enhances transmission of aortic pulsatility. Stroke 2012;43(10):2631.
[93] Hanke M, Baumgartner FJ, Ibe P, Kaule FR, Pollmann S, Speck O, et al. A high-resolution 7-Tesla fMRI dataset from complex natural stimulation with an audio movie. Sci Data 2014:1 140003.
[94] Lahiri S, Schlick KH, Padrick MM, Rinsky B, Gonzalez N, Jones H, et al. Cerebral pulsatility index is elevated in patients with elevated right atrial pressure. J Neuroimaging 2018;28(1):95–8.
[95] Vigen T, Ihle-Hansen H, Lyngbakken MN, Berge T, Thommessen B, Ihle-Hansen H, et al. Carotid atherosclerosis is associated with middle cerebral artery pulsatility index. J Neuroimaging 2020;30(2):233–9.
[96] Tong YJ, Hocke LM, Frederick BD. Short repetition time multiband echo-planar imaging with simultaneous pulse recording allows dynamic imaging of the cardiac pulsation signal. Magn Reson Med 2014;72(5):1268–76.
[97] Kiviniemi V, Wang XD, Korhonen V, Keinanen T, Tuovinen T, Autio J, et al. Ultra-fast magnetic resonance encephalography of physiological brain activity - Glymphatic pulsation mechanisms? J Cereb Blood Flow Metab 2016;36(6):1033–45.
[98] Aslan S, Hocke L, Schwarz N, Frederick B. Extraction of the cardiac waveform from simultaneous multislice fMRI data using slice sorted averaging and a deep learning reconstruction filter. Neuroimage 2019;198:303–16.
[99] Fultz NE, Bonmassar G, Setsompop K, Stickgold RA, Rosen BR, Polimeni JR, et al. Coupled electrophysiological, hemodynamic, and cerebrospinal fluid oscillations in human sleep. Science 2019;366(6465):628-+.
[100] Bock M, Schad LR, Muller E, Lorenz WJ. Pulsewave velocity-measurement using a new real-time MR-method. Magn Reson Imaging 1995;13(1):21–9.
[101] Kaandorp DW, Kopinga K, Wijn PFF. Separation of haemodynamic flow waves measured by MR into forward and backward propagating components. Physiol Meas 1999;20(2):187–99.
[102] Vulliemoz S, Stergiopulos N, Meuli R. Estimation of local aortic elastic properties with MRI. Magn Reson Med 2002;47(4):649–54.
[103] Bouvy WH, Geurts LJ, Kuijf HJ, Luijten PR, Kappelle LJ, Biessels GJ, et al. Assessment of blood flow velocity and pulsatility in cerebral perforating arteries with 7-T quantitative flow MRI. NMR Biomed 2016;29(9):1295–304.
[104] Zarrinkoob L, Ambarki K, Wåhlin A, Birgander R, Carlberg B, Eklund A, et al. Aging alters the dampening of pulsatile blood flow in cerebral arteries. J Cereb Blood Flow Metab 2016;36(9):1519–27.
[105] Geurts LJ, Zwanenburg JJM, Klijn CJM, Luijten PR, Biessels GJ. Higher pulsatility in cerebral perforating arteries in patients with small vessel disease related stroke, a 7T MRI study. Stroke 2019;50(1):62–8.
[106] Vali A, Aristova M, Vakil P, Abdalla R, Prabhakaran S, Markl M, et al. Semi-automated analysis of 4D flow MRI to assess the hemodynamic impact of intracranial atherosclerotic disease. Magn Reson Med 2019;82(2):749–62.
[107] Björnfot C, Garpebring A, Qvarlander S, Malm J, Eklund A, Wåhlin A. Assessing cerebral arterial pulse wave velocity using 4D flow MRI. J Cereb Blood Flow Metab 2021;41(10):2769–77.
[108] Jung JY, Lee YB, Kang CK. Novel technique to measure pulse wave velocity in brain vessels using a fast simultaneous multi-slice excitation magnetic resonance sequence. Sensors-Basel 2021;21(19).
[109] Arts T, Onkenhout LP, Amier RP, van der Geest R, van Harten T, Kappelle J, et al. Non-invasive assessment of damping of blood flow velocity pulsatility in cerebral arteries with MRI. J Magn Reson Imaging 2022;55(6):1785–94.
[110] Markl M, Wallis W, Brendecke S, Simon J, Frydrychowicz A, Harloff A. Estimation of global aortic pulse wave velocity by flow-sensitive 4D MRI. Magn Reson Med 2010;63(6):1575–82.
[111] Rivera-Rivera LA, Cody KA, Rutkowski D, Cary P, Eisenmenger L, Rowley HA, et al. Intracranial vascular flow oscillations in Alzheimer's disease from 4D flow MRI. Neuroimage-Clin 2020:28.

[112] Kim T, Kim SY, Agarwal V, Cohen A, Roush R, Chang YF, et al. Cardiac-induced cerebral pulsatility, brain structure, and cognition in middle and older adults. Neuroimage 2021;233.
[113] Reneman RS, Vanmerode T, Hick P, Muytjens AMM, Hoeks APG. Age-Related-Changes in Carotid-Artery Wall Properties in Men. Ultrasound Med Biol 1986;12 (6):465–71.
[114] Chiesa ST, Masi S, Shipley MJ, Ellins EA, Fraser AG, Hughes AD, et al. Carotid artery wave intensity in mid- to late-life predicts cognitive decline: the Whitehall II study. Eur Heart J 2019;40(28):2300–9.